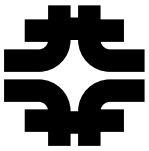

Fermi National Accelerator Laboratory

FERMILAB-Pub-99/141-E
CDF

Search for Technicolor Particles in Lepton Plus Two Jets and Multijet Channels in $p\bar{p}$ Collisions at $\sqrt{s}$ = 1.8 TeV

T. Affolder et al.
The CDF Collaboration

Fermi National Accelerator Laboratory
P.O. Box 500, Batavia, Illinois 60510

May 1999

Submitted to *Physical Review Letters*

Operated by Universities Research Association Inc. under Contract No. DE-AC02-76CH03000 with the United States Department of Energy

Search for Technicolor Particles in Lepton Plus Two Jets and Multijet Channels in $p\overline{p}$ Collisions at $\sqrt{s} = 1.8$ TeV

T. Affolder,[21] H. Akimoto,[42] A. Akopian,[35] M. G. Albrow,[10] P. Amaral,[7] S. R. Amendolia,[31] D. Amidei,[24] J. Antos,[1] G. Apollinari,[35] T. Arisawa,[42] T. Asakawa,[40] W. Ashmanskas,[7] M. Atac,[10] P. Azzi-Bacchetta,[29] N. Bacchetta,[29] M. W. Bailey,[26] S. Bailey,[14] P. de Barbaro,[34] A. Barbaro-Galtieri,[21] V. E. Barnes,[33] B. A. Barnett,[17] M. Barone,[12] G. Bauer,[22] F. Bedeschi,[31] S. Belforte,[39] G. Bellettini,[31] J. Bellinger,[43] D. Benjamin,[9] J. Bensinger,[4] A. Beretvas,[10] J. P. Berge,[10] J. Berryhill,[7] S. Bertolucci,[12] B. Bevensee,[30] A. Bhatti,[35] C. Bigongiari,[31] M. Binkley,[10] D. Bisello,[29] R. E. Blair,[2] C. Blocker,[4] K. Bloom,[24] S. Blusk,[34] A. Bocci,[31] A. Bodek,[34] W. Bokhari,[30] G. Bolla,[33] Y. Bonushkin,[5] D. Bortoletto,[33] J. Boudreau,[32] A. Brandl,[26] S. van den Brink,[17] C. Bromberg,[25] N. Bruner,[26] E. Buckley-Geer,[10] J. Budagov,[8] H. S. Budd,[34] K. Burkett,[14] G. Busetto,[29] A. Byon-Wagner,[10] K. L. Byrum,[2] M. Campbell,[24] A. Caner,[31] W. Carithers,[21] J. Carlson,[24] D. Carlsmith,[43] J. Cassada,[34] A. Castro,[29] D. Cauz,[39] A. Cerri,[31] P. S. Chang,[1] P. T. Chang,[1] J. Chapman,[24] C. Chen,[30] Y. C. Chen,[1] M. -T. Cheng,[1] M. Chertok,[37] G. Chiarelli,[31] I. Chirikov-Zorin,[8] G. Chlachidze,[8] F. Chlebana,[10] L. Christofek,[16] M. L. Chu,[1] S. Cihangir,[10] C. I. Ciobanu,[27] A. G. Clark,[13] M. Cobal,[31] E. Cocca,[31] A. Connolly,[21] J. Conway,[36] J. Cooper,[10] M. Cordelli,[12] J. Guimaraes da Costa,[24] D. Costanzo,[31] D. Cronin-Hennessy,[9] R. Culbertson,[7] D. Dagenhart,[41] F. DeJongh,[10] S. Dell'Agnello,[12] M. Dell'Orso,[31] R. Demina,[10] L. Demortier,[35] M. Deninno,[3] P. F. Derwent,[10] T. Devlin,[36] J. R. Dittmann,[10] S. Donati,[31] J. Done,[37] T. Dorigo,[14] N. Eddy,[16] K. Einsweiler,[21] J. E. Elias,[10] E. Engels, Jr.,[32] W. Erdmann,[10] D. Errede,[16] S. Errede,[16] Q. Fan,[34] R. G. Feild,[44] C. Ferretti,[31] I. Fiori,[3] B. Flaugher,[10] G. W. Foster,[10] M. Franklin,[14] J. Freeman,[10] J. Friedman,[22] H. Frisch,[7] Y. Fukui,[20] S. Galeotti,[31] M. Gallinaro,[35] T. Gao,[30] M. Garcia-Sciveres,[21] A. F. Garfinkel,[33] P. Gatti,[29] C. Gay,[44] S. Geer,[10] D. W. Gerdes,[24] P. Giannetti,[31] P. Giromini,[12] V. Glagolev,[8] M. Gold,[26] J. Goldstein,[10] A. Gordon,[14] A. T. Goshaw,[9] Y. Gotra,[32] K. Goulianos,[35] H. Grassmann,[39] C. Green,[33] L. Groer,[36] C. Grosso-Pilcher,[7] M. Guenther,[33] G. Guillian,[24] R. S. Guo,[1] C. Haber,[21] E. Hafen,[22] S. R. Hahn,[10] C. Hall,[14] T. Handa,[15] R. Handler,[43] W. Hao,[38] F. Happacher,[12] K. Hara,[40] A. D. Hardman,[33] R. M. Harris,[10] F. Hartmann,[18] K. Hatakeyama,[35] J. Hauser,[5] J. Heinrich,[30] A. Heiss,[18] K. D. Hoffman,[33] C. Holck,[30] R. Hollebeek,[30] L. Holloway,[16] R. Hughes,[27] J. Huston,[25] J. Huth,[14] H. Ikeda,[40] M. Incagli,[31] J. Incandela,[10] G. Introzzi,[31] J. Iwai,[42] Y. Iwata,[15] E. James,[24] H. Jensen,[10] M. Jones,[30] U. Joshi,[10] H. Kambara,[13] T. Kamon,[37] T. Kaneko,[40] K. Karr,[41] H. Kasha,[44] Y. Kato,[28] T. A. Keaffaber,[33] K. Kelley,[22] M. Kelly,[24] R. D. Kennedy,[10] R. Kephart,[10] D. Khazins,[9] T. Kikuchi,[40] M. Kirk,[4] B. J. Kim,[19] S. H. Kim,[40] Y. K. Kim,[21] L. Kirsch,[4] S. Klimenko,[11] D. Knoblauch,[18] P. Koehn,[27] A. Köngeter,[18] K. Kondo,[42] J. Konigsberg,[11] K. Kordas,[23] A. Korytov,[11] E. Kovacs,[2] J. Kroll,[30] M. Kruse,[34] S. E. Kuhlmann,[2] K. Kurino,[15] T. Kuwabara,[40] A. T. Laasanen,[33] N. Lai,[7] S. Lami,[35] S. Lammel,[10] J. I. Lamoureux,[4] M. Lancaster,[21] G. Latino,[31] T. LeCompte,[2] A. M. Lee IV,[9] S. Leone,[31] J. D. Lewis,[10] M. Lindgren,[5] T. M. Liss,[16] J. B. Liu,[34] Y. C. Liu,[1] N. Lockyer,[30] M. Loreti,[29] D. Lucchesi,[29] P. Lukens,[10] S. Lusin,[43] J. Lys,[21] R. Madrak,[14] K. Maeshima,[10] P. Maksimovic,[14] L. Malferrari,[3] M. Mangano,[31] M. Mariotti,[29] G. Martignon,[29] A. Martin,[44] J. A. J. Matthews,[26] P. Mazzanti,[3] K. S. McFarland,[34] P. McIntyre,[37] E. McKigney,[30] M. Menguzzato,[29] A. Menzione,[31] E. Meschi,[31] C. Mesropian,[35] C. Miao,[24] T. Miao,[10] R. Miller,[25] S. Miller,[24] H. Minato,[40] S. Miscetti,[12] M. Mishina,[20] N. Moggi,[31] E. Moore,[26] R. Moore,[24] Y. Morita,[20] A. Mukherjee,[10] T. Muller,[18] A. Munar,[31] P. Murat,[31] S. Murgia,[25] M. Musy,[39] J. Nachtman,[5] S. Nahn,[44] H. Nakada,[40] T. Nakaya,[7] I. Nakano,[15] C. Nelson,[10] D. Neuberger,[18] C. Newman-Holmes,[10] C.-Y. P. Ngan,[22] P. Nicolaidi,[39] H. Niu,[4] L. Nodulman,[2] A. Nomerotski,[11] S. H. Oh,[9] T. Ohmoto,[15] T. Ohsugi,[15] R. Oishi,[40] T. Okusawa,[28] J. Olsen,[43] C. Pagliarone,[31] F. Palmonari,[31] R. Paoletti,[31] V. Papadimitriou,[38] S. P. Pappas,[44] A. Parri,[12] D. Partos,[4] J. Patrick,[10] G. Pauletta,[39] M. Paulini,[21] A. Perazzo,[31] L. Pescara,[29] T. J. Phillips,[9] G. Piacentino,[31] K. T. Pitts,[10] R. Plunkett,[10] A. Pompos,[33] L. Pondrom,[43] G. Pope,[32] F. Prokoshin,[8] J. Proudfoot,[2] F. Ptohos,[12] G. Punzi,[31] K. Ragan,[23] D. Reher,[21] A. Ribon,[29] F. Rimondi,[3] L. Ristori,[31] W. J. Robertson,[9] T. Rodrigo,[6] S. Rolli,[41] L. Rosenson,[22] R. Roser,[10] R. Rossin,[29] W. K. Sakumoto,[34] D. Saltzberg,[5] A. Sansoni,[12] L. Santi,[39] H. Sato,[40] P. Schlabach,[10] E. E. Schmidt,[10] M. P. Schmidt,[44] M. Schmitt,[14] L. Scodellaro,[29] A. Scott,[5] A. Scribano,[31] S. Segler,[10] S. Seidel,[26] Y. Seiya,[40] A. Semenov,[8] F. Semeria,[3] T. Shah,[22] M. D. Shapiro,[21] P. F. Shepard,[32] T. Shibayama,[40] M. Shimojima,[40] M. Shochet,[7] J. Siegrist,[21] A. Sill,[38] P. Singh,[16] A. J. Slaughter,[44] K. Sliwa,[41] C. Smith,[17] F. D. Snider,[10] A. Solodsky,[35] J. Spalding,[10] T. Speer,[13] P. Sphicas,[22] F. Spinella,[31] M. Spiropulu,[14] L. Spiegel,[10] L. Stanco,[29] J. Steele,[43] A. Stefanini,[31] J. Strologas,[16] F. Strumia, [13] D.

Stuart,[10] K. Sumorok,[22] T. Suzuki,[40] R. Takashima,[15] K. Takikawa,[40] M. Tanaka,[40] T. Takano,[28] B. Tannenbaum,[5] M. Tecchio,[24] P. K. Teng,[1] K. Terashi,[40] S. Tether,[22] D. Theriot,[10] R. Thurman-Keup,[2] P. Tipton,[34] S. Tkaczyk,[10] K. Tollefson,[34] A. Tollestrup,[10] H. Toyoda,[28] J. F. de Troconiz,[14] S. Truitt,[24] J. Tseng,[22] N. Turini,[31] F. Ukegawa,[40] J. Valls,[36] S. Vejcik III,[10] G. Velev,[31] R. Vidal,[10] R. Vilar,[6] I. Vologouev,[21] D. Vucinic,[22] R. G. Wagner,[2] R. L. Wagner,[10] J. Wahl,[7] N. B. Wallace,[36] A. M. Walsh,[36] C. Wang,[9] C. H. Wang,[1] M. J. Wang,[1] T. Watanabe,[40] T. Watts,[36] R. Webb,[37] H. Wenzel,[18] W. C. Wester III,[10] A. B. Wicklund,[2] E. Wicklund,[10] H. H. Williams,[30] P. Wilson,[10] B. L. Winer,[27] D. Winn,[24] S. Wolbers,[10] D. Wolinski,[24] J. Wolinski,[25] S. Worm,[26] X. Wu,[13] J. Wyss,[31] A. Yagil,[10] W. Yao,[21] G. P. Yeh,[10] P. Yeh,[1] J. Yoh,[10] C. Yosef,[25] T. Yoshida,[28] I. Yu,[19] S. Yu,[30] A. Zanetti,[39] F. Zetti,[21] and S. Zucchelli[3]

(CDF Collaboration)

[1] *Institute of Physics, Academia Sinica, Taipei, Taiwan 11529, Republic of China*
[2] *Argonne National Laboratory, Argonne, Illinois 60439*
[3] *Istituto Nazionale di Fisica Nucleare, University of Bologna, I-40127 Bologna, Italy*
[4] *Brandeis University, Waltham, Massachusetts 02254*
[5] *University of California at Los Angeles, Los Angeles, California 90024*
[6] *Instituto de Fisica de Cantabria, University of Cantabria, 39005 Santander, Spain*
[7] *Enrico Fermi Institute, University of Chicago, Chicago, Illinois 60637*
[8] *Joint Institute for Nuclear Research, RU-141980 Dubna, Russia*
[9] *Duke University, Durham, North Carolina 27708*
[10] *Fermi National Accelerator Laboratory, Batavia, Illinois 60510*
[11] *University of Florida, Gainesville, Florida 32611*
[12] *Laboratori Nazionali di Frascati, Istituto Nazionale di Fisica Nucleare, I-00044 Frascati, Italy*
[13] *University of Geneva, CH-1211 Geneva 4, Switzerland*
[14] *Harvard University, Cambridge, Massachusetts 02138*
[15] *Hiroshima University, Higashi-Hiroshima 724, Japan*
[16] *University of Illinois, Urbana, Illinois 61801*
[17] *The Johns Hopkins University, Baltimore, Maryland 21218*
[18] *Institut für Experimentelle Kernphysik, Universität Karlsruhe, 76128 Karlsruhe, Germany*
[19] *Korean Hadron Collider Laboratory: Kyungpook National University, Taegu 702-701; Seoul National University, Seoul 151-742; and SungKyunKwan University, Suwon 440-746; Korea*
[20] *National Laboratory for High Energy Physics (KEK), Tsukuba, Ibaraki 305, Japan*
[21] *Ernest Orlando Lawrence Berkeley National Laboratory, Berkeley, California 94720*
[22] *Massachusetts Institute of Technology, Cambridge, Massachusetts 02139*
[23] *Institute of Particle Physics: McGill University, Montreal H3A 2T8*
[24] *University of Michigan, Ann Arbor, Michigan 48109*
[25] *Michigan State University, East Lansing, Michigan 48824*
[26] *University of New Mexico, Albuquerque, New Mexico 87131*
[27] *The Ohio State University, Columbus, Ohio 43210*
[28] *Osaka City University, Osaka 588, Japan*
[29] *Universita di Padova, Istituto Nazionale di Fisica Nucleare, Sezione di Padova, I-35131 Padova, Italy*
[30] *University of Pennsylvania, Philadelphia, Pennsylvania 19104*
[31] *Istituto Nazionale di Fisica Nucleare, University and Scuola Normale Superiore of Pisa, I-56100 Pisa, Italy*
[32] *University of Pittsburgh, Pittsburgh, Pennsylvania 15260*
[33] *Purdue University, West Lafayette, Indiana 47907*
[34] *University of Rochester, Rochester, New York 14627*
[35] *Rockefeller University, New York, New York 10021*
[36] *Rutgers University, Piscataway, New Jersey 08855*
[37] *Texas A&M University, College Station, Texas 77843*
[38] *Texas Tech University, Lubbock, Texas 79409*
[39] *Istituto Nazionale di Fisica Nucleare, University of Trieste/ Udine, Italy*
[40] *University of Tsukuba, Tsukuba, Ibaraki 305, Japan*
[41] *Tufts University, Medford, Massachusetts 02155*
[42] *Waseda University, Tokyo 169, Japan*
[43] *University of Wisconsin, Madison, Wisconsin 53706*

[44] *Yale University, New Haven, Connecticut 06520*

We search for color singlet technirho and technipion production in $p\bar{p}$ collisions at $\sqrt{s} = 1.8$ TeV recorded with the Collider Detector at Fermilab. These exotic technimesons are present in a model of walking technicolor. The signatures studied are lepton plus two jets and multijet final states. No excess of events is seen in either final state. We set an upper limit on the technirho production cross section and exclude a region in the technipion mass versus technirho mass plane at the 95% confidence level.

PACS numbers: 13.85.Rm,12.60.Nz,14.80.-j

In the Standard Model, electroweak symmetry breaking is responsible for giving rise to particle masses. The broken symmetry arises from a Higgs scalar field and an as yet unobserved Higgs boson. An alternative explanation for the broken symmetry is through a dynamical interaction known as technicolor [1], where the Higgs boson is replaced by states of two techniquarks, called technipions, bound by the technicolor force. In the walking technicolor (WTC) model [2] color-singlet technirhos ($\rho_T^{\pm,0}$) can be produced in high energy s-channel $q\bar{q}$ annihilation. The decay modes of technirhos are $\rho_T^{\pm} \to W^{\pm}\pi_T^0,\ Z^0\pi_T^{\pm},\ W^{\pm}Z^0,\ \pi_T^0\pi_T^{\pm}$, plus fermion pair ($f\bar{f}'$), and $\rho_T^0 \to W^{\pm}\pi_T^{\mp},\ W^{\pm}W^{\mp},\ \pi_T^{\pm}\pi_T^{\mp}$, plus $f\bar{f}$. The branching ratio of each decay mode depends on the mass of the technirho ($M(\rho_T)$) and the technipion ($M(\pi_T)$). For $M(\pi_T) < \frac{1}{2}M(\rho_T)$, the $\rho_T \to \pi_T\pi_T$ decay dominates. For masses $M(\rho_T) \sim 180\,\mathrm{GeV}/c^2$ and $M(\pi_T) \sim 90$ GeV/c^2, $\rho_T \to W\pi_T$ is the dominant decay mode. The rates of these $\rho_T \to W\pi_T$ and $\rho_T \to \pi_T\pi_T$ decay modes are large enough that we might observe a WTC signal at the Tevatron [3]. The W boson decays to leptonic or hadronic final states, with the leptonic (e or μ) channels having smaller backgrounds. The technipion decays to a pair of fermions. The coupling between a technipion and a fermion is stronger for larger fermion mass. Therefore, a π_T^0 decays mostly to $b\bar{b}$ pairs, and a $\pi_T^{\pm}$ to $\bar{b}c$ [4], producing at least one b-jet. Consequently the $\rho_T \to \pi_T\pi_T$ decay mode produces the only all-hadronic final state with at least two b-jets in this model.

In this analysis, we search for technipions and technirhos in the lepton (e or μ) plus two jets ($\ell+2j$) mode using an integrated luminosity of 109 ± 7 pb^{-1} and in the multijet ($4j$) mode using an integrated luminosity of 91 ± 7 pb^{-1} collected with the Collider Detector at Fermilab (CDF) in 1992-1995. The processes we search for in the $\ell + 2j$ mode are $\rho_T^{\pm,0} \to W^{\pm}\pi_T^{0,\mp} \to \ell\nu b\bar{b}$ or $\ell\nu\bar{b}c$. The main processes we search for in the $4j$ mode are $\rho_T^{\pm,0} \to \pi_T^{\pm}\pi_T^{0,\mp} \to \bar{b}cb\bar{b}$ or $\bar{b}c\bar{b}c$ as well as $\rho_T^{\pm,0} \to W^{\pm}\pi_T^{0,\mp} \to q\bar{q}'b\bar{b}$ or $q\bar{q}'\bar{b}c$. In both modes, we reconstruct technipions from the dijet system where one or both jets are identified ("tagged") as coming from a b hadron. Technirhos are reconstructed from the $W+2$ jet system only in the $\ell+2j$ mode [5].

We describe a counting experiment [6] using the $\ell+2j$ mode, followed by a shape analysis of the dijet invariant mass distribution in both modes. We show cross section limits from both methods. From the $\ell+2j$ mode, we exclude a region in the $M(\pi_T)$ versus $M(\rho_T)$ plane where the $\rho_T \to W\pi_T$ decay mode is dominant. This letter is the first published result in the direct search for color singlet technirho production [7].

The CDF detector [8] consists of a magnetic spectrometer surrounded by calorimeters and muon chambers. A four-layer silicon microstrip vertex detector (SVX) [9], located immediately outside the beam pipe, provides precise track reconstruction in the plane trans-

verse to the beam and is used to identify secondary vertices from b and c hadron decays. The momenta of charged particles are measured in the central tracking chamber (CTC), which is located inside a 1.4-T superconducting solenoid. Outside the CTC, electromagnetic and hadronic calorimeters cover the pseudorapidity region $|\eta| < 4.2$ [10] and are used to identify electron and photon candidates and jets. The calorimeters are also used to determined the missing transverse energy ($\not\!\!E_{\rm T}$), which can indicate the presence of energetic neutrinos. Outside the calorimeters, drift chambers in the region $|\eta| < 1.0$ provide muon identification.

The data selection criteria for the $\ell+2j$ mode is the same as in the Standard Model Higgs boson search analysis in the $W+2$ jet channel [11] plus additional criteria designed to further exploit the characteristics of the WTC signal [3]. We require either an isolated electron with $E_{\rm T} > 20$ GeV or an isolated muon with $P_{\rm T} > 20$ GeV/c in the central region, $|\eta| < 1.0$. We also require $\not\!\!E_{\rm T} > 20$ GeV, and exactly two jets with $E_{\rm T} > 15$ GeV and $|\eta| < 2.0$. Jets are defined as localized energy depositions in the calorimeters and are reconstructed using an iterative clustering algorithm with a fixed cone of radius $\Delta R = \sqrt{\Delta\eta^2 + \Delta\phi^2} = 0.4$ in $\eta - \phi$ space [12]. In order to reduce the large $W+2$ jet background, we require that at least one of the jets be identified as a b-jet candidate. Identification of the b-jet is done by reconstructing secondary vertices from b-quark decay using the SVX (SVX b-tagging). The detail of the SVX b-tagging algorithm is described in Ref. [13]. After the $W+2$ jet with SVX b-tagging selection (Wbq), the observed number of events is 42, while the expected number of background events is 31.6±4.3 (syst) which represents an excess of about 1.5 σ. The major background contributions are $Wb\bar{b}$, $Wc\bar{c}$, and Wc productions. Other backgrounds are due to mistags (tagging a light quark as a b), $t\bar{t}$ and single t production, non-W processes, vector boson pairs, and Z boson plus heavy flavor production.

The acceptance and efficiencies of the signal are estimated using the PYTHIA Monte Carlo [14]. We arbitrarily choose forty-seven mass combinations of the ρ_T and π_T, where the cross sections are larger than ∼5 pb. The model parametes we use are $N_{TC} = 4$ (the number of technicolors, analogous to the three colors in QCD), $Q_D = Q_U - 1 = 1/3$ (techniquarks charges) and sinχ $= 1/3$ (the mixing angle). Details of the parameters are described in [2]. Generated events are passed through a simulation of the CDF detector. The total efficiency of the Wbq selection is approximately 1%, including the branching ratio of $W \to e\nu, \mu\nu$.

We reduce the background further by applying additional selection criteria on the azimuthal angle (ϕ) between the two jets, $\Delta\phi(jj)$, and on the $P_{\rm T}$ of the dijet system, $P_{\rm T}(jj)$, which are unique to this analysis [3]. Our WTC signal search region in the ℓ+2j mode is characterized by $M(\pi_T) + M(W) \simeq M(\rho_T)$. In this case,

technipions are produced nearly at rest in the transverse plane, and consequently the $P_{\rm T}(jj)$ is smaller and the two jets are more back-to-back than in background events. In order to obtain the optimum selection criteria, we apply $\Delta\phi(jj)$ and the $P_{\rm T}(jj)$ requirements simultaneously and maximize the $S/\sqrt{B}$ (signal over square root of the background) values. We thus obtain $\Delta\phi(jj)$ and $P_{\rm T}(jj)$ cut values for each mass combination. For example, at a mass combination of $M(\pi_T) = 90$ GeV/c^2 and $M(\rho_T) = 180$ GeV/c^2, the optimized selection criteria are $\Delta\phi(jj) > 2.1$ and $P_{\rm T}(jj) < 40$ GeV/c. For each mass combination, the efficiency ranges from 80% to 90% for the signal, and 20% to 40% for the background.

We reconstruct the invariant mass of the dijet system, $M(jj)$, which corresponds to the technipion mass, and the invariant mass of the $W+2$ jet system, $M(Wjj)$, which corresponds to the technirho mass. A signal would appear as peaks in the two mass distributions. Jet energy is corrected for calorimeter gaps, non-linear response, energy not contained in the jet cone and underlying event energy. In order to reconstruct the $M(Wjj)$, we need to estimate the $P_{\rm z}$ of the neutrino ($P_{\rm z}(\nu)$) which is unknown since we measure only its transverse component. We solve for $P_{\rm z}(\nu)$ using the W mass constraint in a lepton-neutrino system and take the smaller $|P_{\rm z}(\nu)|$ of the two solutions [15]. If there is no real solution for the $P_{\rm z}(\nu)$, we take the real part of the solution of the quadratic equation. Figure 1 shows the $M(jj)$ and $M(Wjj)$ distributions before and after the $\Delta\phi(jj)$ and $P_T(jj)$ requirements for data and simulation for $M(\pi_T) = 90$ GeV/c^2 and $M(\rho_T) = 180$ GeV/c^2. Finally, we apply a mass window requirements. The signal Monte Carlo sample is used to estimate the mean and resolution (σ_m) for each $M(jj)$ and $M(Wjj)$. We define the mass window requirement to be within $\pm 3\sigma_m$ of the mean mass value. The typical mass resolutions for $M(jj)$ and $M(Wjj)$ are approximately 15 GeV/c^2 and 20 GeV/c^2, respectively.

Table I summarizes our results. The small excess seen in the $\ell + 2j$ mode after the Wbq selection is no longer present after the cuts designed to enhance a contribution from WTC. We set 95% C.L. upper limits on $\sigma_{counting}$, taking into account a total 27% systematic uncertainty in the efficiency. The $\sigma_{counting}$ is defined as $\sigma(p\bar{p} \rightarrow \rho_T \rightarrow W\pi_T)$ times the branching ratio (BR), where BR includes $\pi_T^0 \rightarrow b\bar{b}$ and $\pi_T^{\pm} \rightarrow \bar{b}c$. The dominant sources of systematic uncertainty are initial state radiation (10%) and final state radiation (19%). We exclude a region in the $M(\pi_T)$ versus $M(\rho_T)$ plane as shown in Figure 2.

We now describe a search for technipions using the dijet mass distributions of two b-tagged jets in the ℓ+2j and $4j$ channels. The $4j$ channel is senstive to both the $W\pi_T$ and $\pi_T\pi_T$ decays of the ρ_T, while the $\ell+2j$ analysis described above searched for $\rho_T \rightarrow W\pi_T$ decays only. This analysis is similar to a previous published CDF search for Standard Model Higgs boson production in association

with a W boson [16], but has improved the sensitivity for this technipion search [17]. We chose a grid of points in the $M(\rho_T)$ versus $M(\pi_T)$ plane outside the region already excluded by the counting experiment. This dijet mass shape study sets cross section limits by searching directly for a narrow technipion decay and therefore complements our search using the counting experiment.

The multijet data sample is the same as [16]. Events are required to have four or more jets with $E_{\rm T} > 15$ GeV and $|\eta| < 2.1$. In addition, we require that at least two of the four highest E_T jets in the event be identified as b quark candidates to reduce the large QCD background. Only the four highest $E_{\rm T}$ jets are considered for the mass reconstruction: the two highest $E_{\rm T}$ b-tagged jets are assigned to the technipion, and the other two to the vector boson or the other technipion. A further selection criterion, which is unique to this analysis, is imposed on the ϕ angle between the two highest $E_{\rm T}$ b-tagged jets, $\Delta\phi(b\bar{b}) \geq 1.5$, to remove the gluon splitting component of the background and to reduce the wrong jet assignments that may arise when more than one technipion is present.

We observe 389 events in data after all the selection requirements are applied. The main source of background is QCD heavy flavor ($b\bar{b}/c\bar{c}$) production for which the normalization is not well known and is left free in the fit. Other backgrounds are $t\bar{t}$, Z + jets with $Z \to b\bar{b}/c\bar{c}$, and mistags. These non-QCD backgrounds are estimated to be 114±12 (syst) events. The total signal efficiency varies from 0.2% to 0.5% depending on the π_T and ρ_T masses. This efficiency is primarily a result of the high energy threshold of the multijet trigger (∼2% to ∼8%) and the double-b-tag requirement (∼10%). The trigger efficiency falls at lower ρ_T mass region where $\rho_T \to \pi_T\pi_T$ cross section is higher. Figure 3 shows invariant mass distribution of the b-tagged dijet system for data, background and $M(\pi_T) = 95$ GeV/c^2 and $M(\rho_T) = 195$ GeV/c^2 signal. We use the same method as in Ref. [16] and place limits on $\sigma_{fitting}$ by taking into account a 34% total systematic uncertainty in the efficiency and shape. The $\sigma_{fitting}$ is defined as $\sigma(p\bar{p} \to \rho_T \to WW, WZ, W\pi_T, Z\pi_T, \pi_T\pi_T)$ times BR, where BR includes $W/Z \to jj$, $\pi_T^0 \to b\bar{b}$ and $\pi_T^{\pm} \to \bar{b}c$. We apply the same fitting procedure to the ℓ+2j data sample. The $\Delta\phi(jj)$ and $P_{\rm T}(jj)$ requirements are not applied in order to have sufficient statistics to fit the dijet mass distribution.

Table II summarizes the result from the shape analysis which provides no further constraint to the WTC model. However, in addition to the limits on $\sigma_{fitting}$, the results provide us important guidance for the upcoming Tevatron run. Besides higher luminosity and significant detector improvements, we will have the ability to trigger on hadronic b decays by way of charged track impact parameter information. This hadronic b trigger along with lower trigger energy thresholds will significantly improve our sensitivity to technicolor models.

In summary, we have performed a search for technicolor particles, ρ_T and π_T. From the counting experiment in the $\ell+2j$ mode with $\Delta\phi(jj)$, $P_{\rm T}(jj)$, and mass window cuts, no excess over background estimation is observed, and we set production cross section limits. We exclude a region in the $M(\rho_T)$ and $M(\pi_T)$ plane at the 95% C.L. We also performe a search using the shape of the dijet invariant mass distributions in the $4j$ and the $\ell+2j$ modes and set cross section limits.

We thank K. Lane for stimulating discussions and for his contribution to the theoretical interpretation and S. Mrenna for incorporating the WTC model in the PYTHIA Monte Carlo. We thank the Fermilab staff and the technical staffs of the participating institutions for their vital contributions. This work was supported by the U.S. Department of Energy and National Science Foundation; the Italian Istituto Nazionale di Fisica Nucleare; the Ministry of Education, Science and Culture of Japan; the Natural Sciences and Engineering Research Council of Canada; the National Science Council of the Republic of China; the A. P. Sloan Foundation; and the Swiss National Science Foundation.

---

[1] S.Weinberg, Phys. Rev. D **13**, 974(1976); **19**, 1277 (1979); L. Susskind, Phys. Rev. D **20**, 2619 (1979).
[2] E. Eichten and K. Lane, Phys. Lett. B **388**, 803 (1996), and references therein.
[3] E. Eichten, K. Lane, and J. Womersley, Phys. Lett. B **405**, 305 (1997).
[4] The $\bar{b}c$ represents either $b\bar{c}$ or $\bar{b}c$.
[5] The high ΣE_T threshold (125 GeV) of the multijet trigger prevents us from looking for a ρ_T peak in the 4-jet invariant mass distribution in the $4j$ mode.
[6] See Particle Data Group, R. Barnett *et al.*, Phys. Rev. D**54**, 1 (1996), Sec. 28.6.4.
[7] We recently submitted a paper FERMILAB-PUB-98/321-E, *"Search for a Technicolor ω_T Particle in Events with a Photon and a b-quark Jet at CDF"* to Phys. Rev. Lett. October 9, 1998.
[8] F. Abe *et al.*, Nucl. Instrum. Methods Phys. Res., Sect. A **271**, 387 (1988).
[9] D. Amidei *et al.*, Nucl. Instrum. Methods Phys. Res., Sect. A **350**, 73 (1994).
[10] In CDF the positive z (longitudinal) axis lies along the proton beam direction, r is the radius from this axis, θ is the polar angle and ϕ is the azimuthal angle. Pseudorapidity (η) is defined as $\eta \equiv -\ln(\tan(\theta/2))$. "Transverse momentum" ($P_{\rm T}$) and "transverse energy" ($E_{\rm T}$) are the momentum and energy flow measured transverse to the beam line, respectively. The "missing transverse" ($\not\!\!E_{\rm T}$) is defined as $-\Sigma E_T^i \hat{r}_i$, where $\hat{r}_i$ is a unit vector in the transverse plane pointing to the center of the calorimeter tower i and E_T^i is the transverse energy deposited in that tower. Only towers with $|\eta| \geq 3.6$ are included.
[11] F. Abe *et al.*, Phys. Rev. Lett. **79**, 3819 (1997).
[12] F. Abe *et al.*, Phys. Rev. D **45**, 1448 (1992).
[13] F. Abe *et al.*, Phys. Rev. Lett. **79**, 1992 (1997).
[14] T. Sjöstrand, Comput. Phys. Commun. **82**, 74(1994). We use version 6.1.
[15] Monte Carlo studies show that the smaller $|P_z|$ solution is closer to the generated neutrino $\sim 60\%$, the larger $|P_z|$ solution $\sim 30\%$ and there is no real solution $\sim 10\%$ of the times.
[16] F. Abe *et al.*, Phys. Rev. Lett. **81**, 5748 (1998).
[17] In addition, we have improved our estimation of the multijet trigger efficiency using a control sample of QCD jet events.

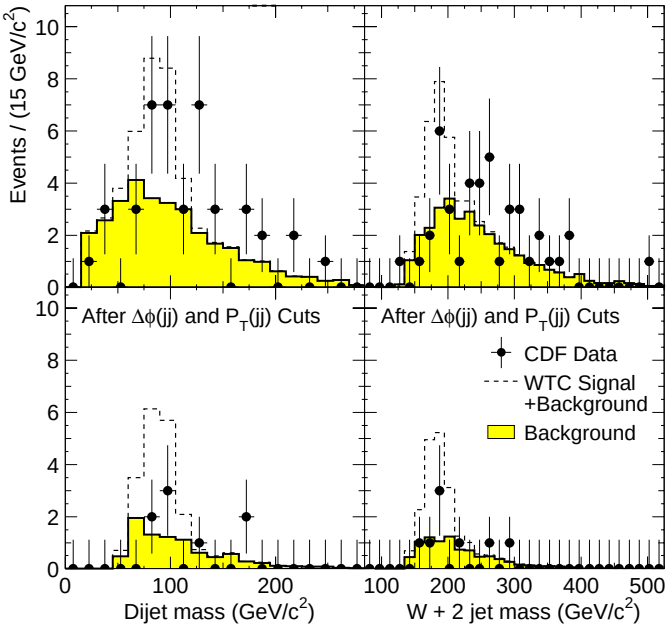

FIG. 1. The invariant mass of the dijet system and of the $W+2$jet system for the $\ell+2j$ mode. Requirements of $\Delta\phi(jj) > 2.1$ and $P_{\rm T}(jj) < 40$ GeV/c are applied in the bottom plots. The number of events of the background and the technicolor Monte Carlo signal are normalized to the expected number of events in 109 pb^{-1}. The mass combination shown is $M(\pi_T)$=90 GeV/c^2 and $M(\rho_T)$=180 GeV/c^2.

$M_{(\pi_T,\rho_T)}$ [GeV/c^2]	$\sigma^{theory}_{counting}$ [pb]	$\epsilon_{tot.}$ [%]	$N_{exp.}$	$N_{B.G.}$	$N_{obs.}$	$N_{lim.}$	$\sigma^{lim.}_{counting}$ [pb]
80,170	3.7	0.64	2.6	5.4±0.7	5	7.3	10.5
85,170	14.1	0.66	10.2	3.8±0.5	5	8.4	11.7
90,180	15.7	0.69	11.8	5.7±0.8	5	7.1	9.5
95,185	13.0	0.88	12.5	6.4±0.9	6	7.9	8.1
100,190	10.9	0.92	10.9	6.5±0.9	6	7.8	7.8
105,200	9.3	0.94	9.5	7.4±1.0	8	9.5	9.2
110,210	7.4	0.97	7.9	9.8±1.3	13	13.8	13.0
115,210	6.9	1.02	7.7	8.4±1.2	10	11.2	10.0

TABLE I. Summary of the $\ell+2j$ mode counting experiment for various π_T and ρ_T mass combinations after all selection cuts have been applied. The $\sigma^{theory}_{counting}$ is the expected theoretical $\sigma_{counting}$. The $\epsilon_{tot.}$ is the total efficiency, $N_{exp.}$ is the expected number of signal events, $N_{B.G.}$ is the estimated number of background events, $N_{obs.}$ is the observed number of events, and $N_{lim.}$ and $\sigma^{lim.}_{counting}$ are the 95% C.L. limits, taking into account a 27% systematic uncertainty.

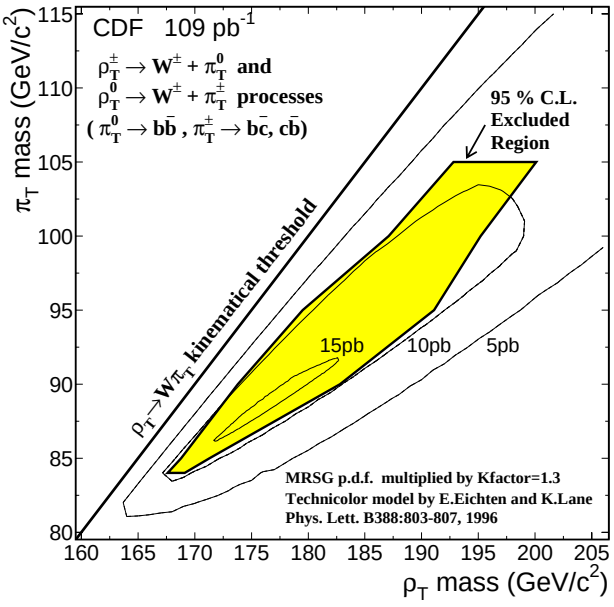

FIG. 2. The shaded region shows the 95% C.L. excluded region in the $M(\pi_T)$, $M(\rho_T)$ plane. Three contours of $\sigma^{theory}_{counting}$ are also shown (5,10, and 15 pb). PYTHIA v6.1 with MRSG parton distribution function and a K-factor =1.3 is used to calculate the cross section.

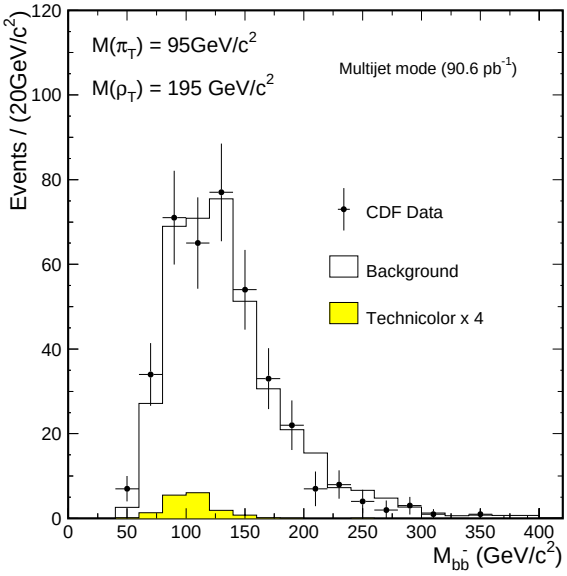

FIG. 3. Invariant mass distribution of the b-tagged dijet system for the $4j$ mode. The number of background events is normalized to data, and the number of expected events for the technicolor signal is normalized to the expected number of events in 90.6 pb^{-1} times 4. The mass combination used is $M(\pi_T)$=95 GeV/c^2 and $M(\rho_T)$=195 GeV/c^2.

		95% C.L. upper limits on $\sigma_{fitting}$		
$M_{(\pi_T,\rho_T)}$ [GeV/c^2]	$\sigma_{fitting}^{theory}$ [pb]	$4j$ [pb]	ℓ+$2j$ [pb]	Combined [pb]
95,195	12.3	613	50.1	160
100,205	9.8	257	44.2	109
105,205	8.2	375	31.1	82
110,210	7.3	388	31.5	83
110,220	6.6	362	32.0	89

TABLE II. 95% C.L. upper limits on $\sigma_{fitting}$ from the two different channels and from their combination. The first column lists the mass combinations, the second is the theoretical cross section, the third, fourth and fifth column are the 95% C.L. limits from the $4j$, ℓ+$2j$ and combination of both, respectively. We note here that $\sigma_{fitting}$ includes the $W/Z \rightarrow jj$ branching ratio.